Coaxial Electromagnetic Launcher Calculations Using FE-BE Method and Hybrid Potentials

J.H. Chang, E.B. Becker
Department of Aerospace Engineering and Engineering Mechanics
The University of Texas at Austin
Austin, Texas 78712

M.D. Driga
Institute for Advanced Technology
The University of Texas at Austin
Austin, Texas 78759

***Abstract*—In this paper, a hybrid method combining finite and boundary elements (the FE-BE method) is presented to analyze the transient electromagnetic /mechanical behavior of coaxial induction launchers (i.e., the coilgun). The corresponding initial/boundary value problem is formulated in terms of the hybrid potentials, which mixes the vector and scalar magnetic potential functions. The problem is assumed to be axisymmetric and the forcing currents are circumferential. Thermal effect due to ohmic losses is considered during the launching processes.**

I. INTRODUCTION

Lately, the increased attention to the induction coil launchers has promoted the publication of a number of numerical models for their analysis and design; e.g., the cylindrical current sheet model [1], the current filament method [2], and the circuit approach [3]. In these models, the conductors were simulated with either current sheets or filaments. In this paper, a comprehensive model combining the FE-BE methods is developed for more advanced and efficient study on the transient behavior.

In practice, the FE method is a robust general approximation process. However, it is difficult to model a physical system with infinite domain, which occurs in many of the electromagnetic problems. To overcome these difficulties we use the boundary elements, which represent the exterior infinite region, in conjunction with the finite elements, which solve the complex problem in the near domain. The concept of this hybrid FE-BE method was used in several applications for magnetostatic field analysis [4, 5] and eddy current problems [6].

The launching problem is seldom treated in detail because of the difficulty of adaptation of the finite element mesh to the complex change in fields and mechanical positions of the stator and the projectile. With the hybrid FE-BE method, this moving mesh is easy to deal with if the moving body is modeled with finite elements and enclosed by boundary element contours. This part of mesh then adheres to the body and moves with it.

The corresponding electromagnetic problems are formulated in terms of the magnetic potential functions. To minimize the set of degrees of freedom and to maintain numerical stability simultaneously, the method of hybrid potential [7] is used. The concept is to use the vector potential pair $\vec{A}$ and ψ in the conducting area and a magnetic scalar potential ϕ elsewhere, with the interface consistent with the conductor surface.

The problem is assumed to be axisymmetric. Fig. 1 illustrates a typical problem geometry. In this figure, Ω_1 denotes the subdomain occupied by the field coils, while Ω_2 and Ω_3 are the regions occupied by the air and the moving projectile, respectively. In the present formulation hysteresis, displacement currents, polarization, and free space charges are neglected. All parts constituting the device are assumed to be rigid.

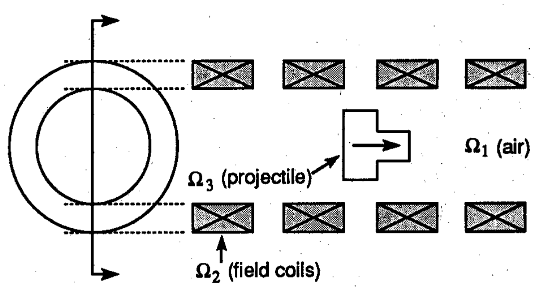

Fig. 1: The typical problem geometry of a multi-stage coaxial Electromagnetic launcher.

Temperature rise due to ohmic losses is considered with the assumption that the ohmic losses dissipate adiabatically in the conductors. The assumption is reasonable for the relatively short duration of launching process (~ 10^{-3}/s).

Together with various special numerical treatments [8, 9], a computer program TEXCAL (Texas Electromagnetic Coaxial Launcher Analysis Code) was developed for this analysis. Two example problems are presented, along with the numerical results generated by TEXCAL.

II. GOVERNING EQUATIONS

Two sets of governing equations are involved in this problem. The first one is associated with the electromagnetic field. With the previous assumptions, we have:

0018-9464/93$03.00

Simplified Maxwell's Equations

$$\nabla \times \vec{H} = \vec{J} \tag{1}$$

$$\nabla \times \vec{E} = -\frac{\partial \vec{B}}{\partial t} + \nabla \times \left(\vec{v} \times \vec{B}\right) \tag{2}$$

$$\nabla \cdot \vec{B} = 0 \tag{3}$$

Continuity Equation

$$\nabla \cdot \vec{J} = 0 \tag{4}$$

Constitutive Law

$$\vec{B} = \mu\left(\vec{H}\right) \vec{H} \tag{5}$$

Ohm's Law

$$\vec{J} = \sigma\left(T\right) \vec{E} \tag{6}$$

where $\vec{H}, \vec{J}, \vec{E}, \vec{B}, \vec{v}, \mu, \sigma, T$ are magnetic field intensity, current density, electric field intensity, magnetic flux density, velocity vector, permeability, conductivity and temperature, respectively. The second term on the right-hand side of (2), $\nabla \times \left(\vec{v} \times \vec{B}\right)$, accounts for the moving behavior of the projectile and may have a nonzero value when the *spatial description* is used.

When there is no source current along the interface between two different materials, the following boundary conditions must hold:

$$\vec{B}_1 \cdot \vec{n}_1 + \vec{B}_2 \cdot \vec{n}_2 = 0 \tag{7}$$

$$\vec{H}_1 \times \vec{n}_1 + \vec{H}_2 \times \vec{n}_2 = \vec{0} \tag{8}$$

where the subscripts 1 and 2 denote the material numbers, $\vec{n}_i$ is the outward unit normal for material i along the interface.

The second set of governing equations deals with the motion of the concluding projectile. Due to the axisymmetric assumption, the only nonvanishing components of the velocity vector are the axial linear velocity and the spinning component. Usually the spinning component is used only to provide gyroscopic stability for the projectile during post-launch flight [10], and so is not considered in this paper.

From the Newton's Law, we obtain the equation of motion

$$M \frac{dv_z}{dt} \vec{e}_z = \int_{\Omega_3} \left(\vec{J} \times \vec{B}\right)_z d\Omega \tag{9}$$

where M is the mass of the moving body which occupies domain Ω_3, v_z is the linear velocity in the axial direction z. The integrand in the equation, $\vec{J} \times \vec{B}$ is the Lorentz force, with the subscript z denoting the component in the axial direction.

III. THE HYBRID POTENTIALS

A general formulation of the potential function for the electromagnetic field calculation is the four component vector including the magnetic vector potential $\vec{A}$ and an electric scalar potential v. For the axisymmetric case with the source current flowing invariantly in the circumferential direction, and the axial linear motion as the only moving component of the projectile, the problem reduces to the solution of one component of the magnetic vector potential A_θ.

The magnetic scalar potential ϕ is used in the area where no eddy current occurs. For most problems, the current-carrying conductors occupy a relatively small fraction of the total region. It is evident that the introduction of ϕ does greatly reduce the effort in computation. However, this scalar potential is not a single-valued function of position when the region in which ϕ is defined is multiply connected. A solution to this problem is to turn the scalar region into a simply connected one by introducing the $\vec{A}$ *regions* [11] spanning the holes in the conductors, where the $\vec{A}$ regions denote the nonconducting subareas modeled in terms of the magnetic vector potential. For the problem in Fig. 1, a set of $\vec{A}$ regions is introduced and shown as the shaded areas in Fig. 2.

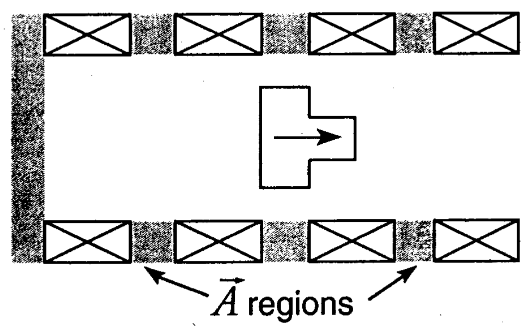

Fig. 2. A set of $\vec{A}$ regions are introduced to turn the relevant region into a simply connected one.

By using this concept of hybrid potentials, the problem is then formulated in terms of the magnetic vector potential in both the conducting areas and the $\vec{A}$ regions, and the magnetic scalar potential elsewhere. Therefore, in Ω_i (i = 1, 3), and the $\vec{A}$ regions

$$\sigma\frac{\partial A_\theta}{\partial t} - \nabla\cdot\frac{1}{\mu}\nabla A_\theta + \frac{1}{\mu}\frac{1}{r^2}A_\theta = J_2 \tag{10}$$

where $J_q = 0$ in Ω_3, and the $\vec{A}$ regions. In $\Omega_2 - \{\vec{A}\text{ regions}\}$,

$$\nabla\cdot\frac{1}{\mu_o}\nabla\phi = 0 \tag{11}$$

These two sets of potential functions A_θ and ϕ are related by the boundary conditions along the interface

$$-\mu_0\left(\nabla\phi\cdot\vec{n}\right) = \nabla\times A_\theta\vec{e}_\theta\cdot\vec{n} \tag{12}$$

$$-\nabla\phi\times\vec{n} = \frac{1}{\mu}\nabla\times A_\theta\vec{e}_\theta\times\vec{n} \tag{13}$$

where $\vec{n}$ is defined as the outward unit normal to the surface of Ω_2.

The axial velocity v_z does not appear in the above equations because the *material description* is used in characterizing the axial movement.

With the above formulations, the hybrid FE-BE method is then applicable. As shown in Fig. 3, the shaded areas, i.e., the field coils, moving body, and $\vec{A}$ regions are represented by finite elements. The open region, the air, is represented by boundary elements. The boundary element contours, consistent with the material interface, are shown as dashed lines.

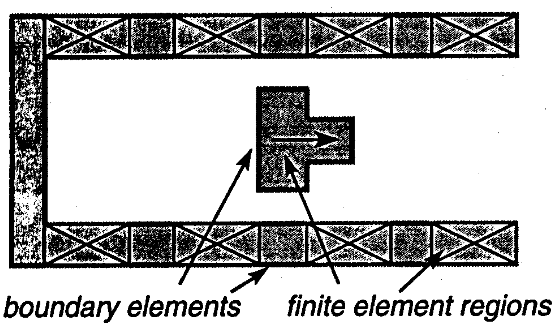

Fig. 3: An application of the FE-BE hybrid method to the problem.

IV. SIMULATION OF A SINGLE-STAGE INDUCTION LAUNCHER

This example is chosen to demonstrate the capability of TEXCAL. The problem is similar to the one considered in [2]. Fig. 4 shows the initial geometrical configuration of the cross section of the device in the r - z plane. This launcher device consists of a field coil, which is made of 10 turns of 60% packing copper litz, and a monolithic single-turn armature assembly mainly made of aluminum.

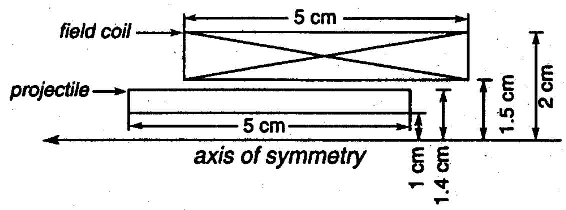

Fig. 4: The initial configuration for the single-stage launcher.

As shown in Fig. 5, the field coil was modeled with 10 parallel coaxial current filaments while 19 filaments were used for the armature. A FE-BE mesh of linear elements, as shown in Fig. 6, is constructed here to simulate this current filament model with 10 and 19 finite elements for the coil and armature, respectively. The extra finite elements in this model account for the $\vec{A}$ regions. For those data not revealed in [2], values were inferred from other sources [12-13].

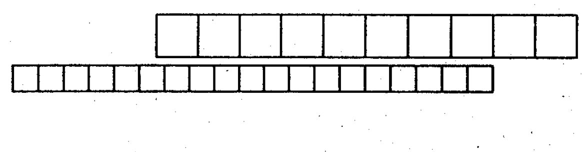

Fig. 5: The filament model.

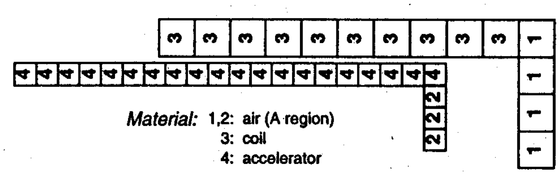

Fig. 6: The FE-BE model simulating the filament model.

Fig. 7 and Fig. 8 present a comparison of the solutions obtained from the FE-BE and filament models at time 0.0155 ms, at which the input current reaches its peak value. Shown in Fig. 7 are the eddy current distributions versus the axial position in the projectile. The corresponding temperature distributions are shown in Fig. 8. Shown in Fig. 9 is the normalized velocity of the projectile versus time, along with the values of input current density in the field coil.

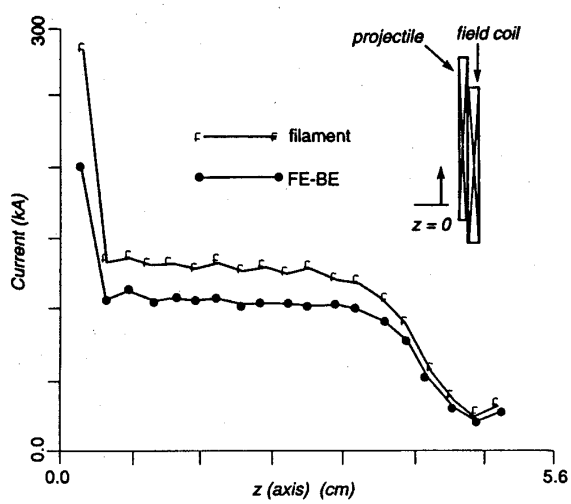

Fig. 7: The eddy current distributions vs. the axial positions in the launcher from the two models at time 0.0155 ms.

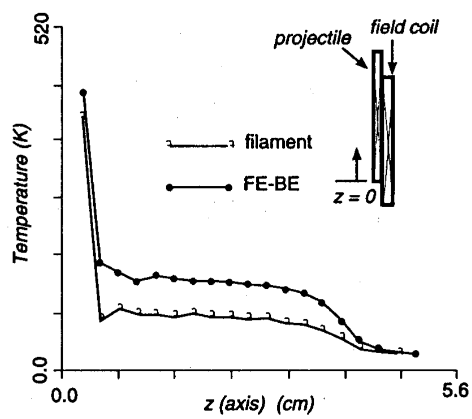

Fig. 8: The temperature distributions vs. the axial position in the launcher from the two models at time 0.0155 ms.

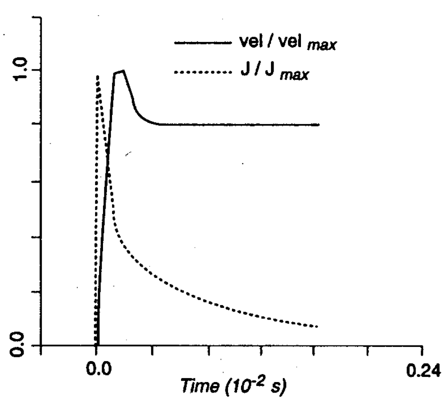

Fig. 9. The normalized values of input current density and velocity vs. time.

Due to possible discrepancies in the data, the results from the FE-BE and the filament models would not be expected to match exactly. However, they so far appear to show good agreement in the trend of the solutions.

V. SIMULATION OF A FIVE-STAGE LAUNCHER

To accelerate the projectile up to a hypervelocity, a multi-stage launcher device is necessary.

In this example, a five-stage launcher is simulated. Each coil in this system has its own capacitor power bank which is turned on by using some 'sense and switch' approach. Through the sensors, the rise time of the coil is determined upon arrival of the launcher so that correct timing of the power discharge at each stage is ensured. A 5 kg aluminum projectile is accelerated in the field produced by the five coils located to one another with a spacing of 1.07 cm. The feature of sense and switch is incorporated into TEXCAL so that each coil is turned on when the projectile reaches a certain position. Fig. 10 shows the cross section and FE-BE model of the device at its initial position.

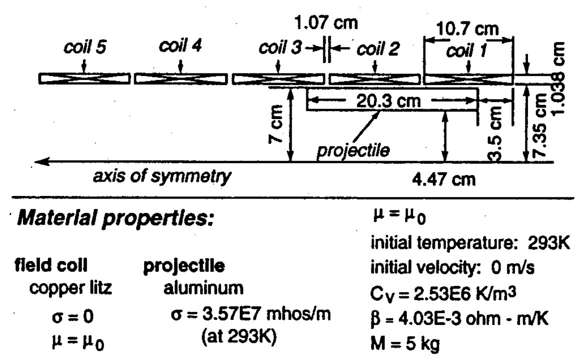

Fig. 10. The initial geometrical configuration of the five-stage launcher in the r-z plane.

Fig. 11 illustrates the distribution of input current density in the five coils versus time. The launching process generates a maximum peak acceleration of 1.64×10^6 m/s^2 at the fourth stage and final velocity of 553 m/s. Fig. 12 shows time distribution of the normalized values of the velocity and acceleration. Fig. 13 shows configurations of the mesh at the second and third stages, with the armature located at the corresponding firing positions.

The shaded area shown in Fig. 14 indicates that 5% of the projectile is of temperature higher than the melting point at the end of launching.

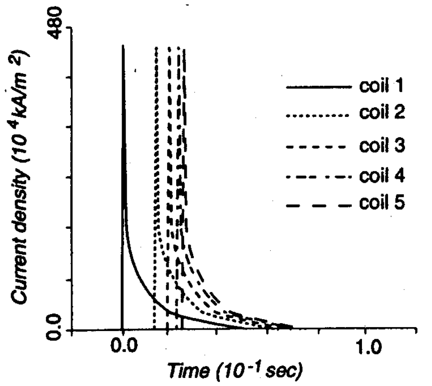

Fig. 11. **The distribution of current density vs. time in the five coils.**

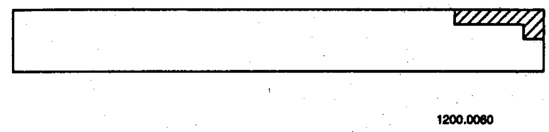

Fig. 14. **The shaded area indicates the portion of the projectile with final temperature higher than melting point.**

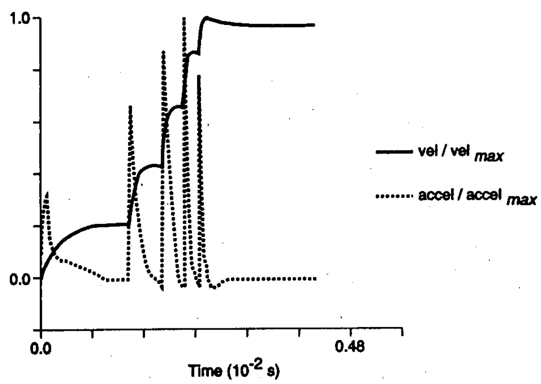

Fig. 12. **Time distribution of normalized values of the velocity and acceleration.**

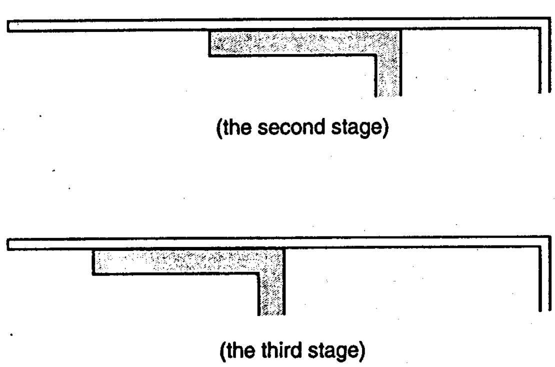

Fig. 13. **Configurations of the mesh at the firing positions of the second and third stages.**

VI. CONCLUSIONS

A numerical model which simulates the transient behavior of a coaxial electromagnetic launcher was developed in this research. Two main 'hybrid' features were included in the model. The problem is first formulated in terms of the combination of magnetic scalar and vector potentials, with the vector potential applied in the conducting region and the scalar potential in the infinite nonconducting area (i.e., the air). The resulting initial/boundary value problem is then discretized by dividing these two subareas into a number of finite and boundary elements. The model is effective in characterizing the moving behavior of this problem.

ACKNOWLEDGMENT

The support of this research by the Institute for Advanced Technology, a Federally Funded Research and Development Center (FFRDC) for the U.S. Army, is greatly appreciated.

REFERENCES

[1] J. L. He, Z. Zabar, E. Levi, and L. Birenbaum, "Analysis of induction-type coilgun performance based on cylindrical current sheet model," *IEEE Trans. Magn.*, vol. 27, no. 1, pp. 379-584, January 1991.

[2] J. A. Andrews and J.R. Devine, "Armature design for coaxial induction launchers," *IEEE Trans. Magn.*, vol. 27, no. 1, pp. 639-643, January 1991.

[3] M .M. Widner, "WARP-10: A numerical simulation model for the cylindrical reconnection launcher," *IEEE Trans. Magn.*, vol. 27, no. 1, pp. 634-638, January 1991.

[4] S. Christine and A. Di Napoli, "Combination of finite and boundary elements for magnetic field analysis," *IEEE Trans. Magn.*, vol. Mag-19 no. 6, pp. 2337-2339, November 1983.

[5] S .J. Salon and J. D'Angelo, "Applications of the hybrid finite element-boundary element method in electromagnetics," *IEEE Trans. Magn.*, vol. 24, no. 1, pp. 80-85, January 1988.

[6] F. Matsuoka and A. Kameari, "Calculation of three dimensional eddy current by FEM-BEM coupling method," *IEEE Trans. Magn.*, vol. 24, no. 1, pp. 182-185, January 1988.

[7] T. Onuki, A. Ishiyama, T. Abe and Y. Murrai, "Hybrid finite-boundary element method using vector and scalar potentials for open boundary magnetic field problem," *Proc. 5th Intl. Conf., Hiroshima, Japan*, pp. 113-122, November 1983.

[8] S. J. Polak, A. J. H. Wachters and J S. van Welijj, "A new 3-D eddy current model," *IEEE Trans. Magn.*, vol. Mag-19, no. 6, pp. 2447-2449, November 1983.

[9] J .H. Chang, *Numerical Simulation for Coaxial Electromagnetic Launcher by Using FE-BE Method with Hybrid Potentials*, Ph.D., dissertation., The University of Texas at Austin, May 1992.

[10] R. J. Kaye, et. al., "Design and performance of a multi-stage cylindrical reconnection launcher," *IEEE Trans. Magn.*, vol. 27, no. 1, pp. 596-600, January 1991.

[11] D. Rodgers and J. F. Estham, "Multiply connected regions in the three dimensional eddy current formulation," *IEEE Proc.*, vol. 134, pt. A, no. 1, pp. 58-66, January 1987.

[12] M. W. Ingram, J .A. Andrews and D .A. Bresie, "An actively switched pulsed induction accelerator," *IEEE Trans. Magn.*, vol. 27, no. 1, pp. 591-595, January 1991.

[13] H. Knoepfel, *Pulsed High Magnetic Fields*, North-Holland Publishing Company, 1970.